Upwelling O+ ion source characteristics

Article

Published Version

JOURNAL OF GEOPHYSICAL RESEARCH, VOL. 91, NO. A6, PAGES 7019–7031, JUNE 1, 1986

Upwelling O^+ Ion Source Characteristics

T. E. MOORE,[1] M. LOCKWOOD,[2] M. O. CHANDLER,[3] J. H. WAITE, JR.,[1]
C. R. CHAPPELL,[1] A. PERSOON,[4] AND M. SUGIURA[5]

Recent observations from the Dynamics Explorer 1 (DE 1) spacecraft have shown that the dayside auroral zone is an important source of very low-energy superthermal O^+ ions for the polar magnetosphere. When observed at 2000- to 5000-km altitude, the core of the O^+ distribution exhibits transverse heating to energies on the order of 10 eV, significant upward heat flux, and subsonic upward flow at significant flux levels (exceeding 10^8 cm^{-2} s^{-1}). The term "upwelling ions" has been adopted to label these flows, which stand out in sharp contrast to the light ion polar wind flows observed in the same altitude range in the polar cap and subauroral magnetosphere. We have chosen a typical upwelling ion event for detailed study, correlating retarding ion mass spectrometer observations of the low-energy plasma with energetic ion observations and local electromagnetic field observations. The upwelling ion signature is colocated with the magnetospheric cleft as marked by precipitating energetic magnetosheath ions. The apparent ionospheric heating is clearly linked with the magnetic field signatures of strong field-aligned currents in the vicinity of the dayside polar cap boundary. Electric field and ion plasma measurements indicate that a very strong and localized convection channel or jet exists coincident with the other signatures of this event. These observations indicate that transverse ion heating to temperatures on the order of 10^5 K in the 2000- to 5000-km ionosphere is an important factor in producing heavy ion outflows into the polar magnetosphere. This result contrasts with recent suggestions that electron heating (to temperatures of order 10^4 K) is the most important parameter with regard to O^+ outflow.

INTRODUCTION

Evidence for a poleward dispersion in mass, pitch angle, and energy of solar wind particles entering the cusp/magnetopause boundary is a well-documented phenomenon [cf. *Burch et al.*, 1982; *Peterson*, 1985]. The ordered ion dispersion signature is the result of a localized cusp injection point near the magnetopause boundary and the subsequent time of flight spreading of the ions due to the action of high-latitude $E \times B$ convection. Recent measurements of low-energy ionospheric ions by the Dynamics Explorer 1 satellite (DE 1) have revealed similar dispersion in both mass and energy of the out-flowing plasma from the cusp region ionosphere.

In addition, observations from DE 1 have revealed low-energy ion outflows in the polar magnetosphere [*Shelley et al.*, 1982; *Gurgiolo and Burch*, 1982]. Using electric field data from the sister DE 2 satellite, *Waite et al.* [1985] found that such flows originated in a dayside source or energization region and were convected antisunward to observing points within the polar cap. *Moore et al.* [1985] showed that a localized ionospheric heating signature was characteristic of the dayside auroral zone while *Lockwood et al.* [1985*a*] found, from a statistical study of such events, that such a source of O^+ ions is persistently present in the prenoon sector of the dayside polar cap boundary or auroral zone and suggested that this was the dominant source of heavy ions for the polar cap magnetosphere. The term "upwelling ions" was used to refer to these events, and it was suggested that they are the source region for the field-aligned polar cap O^+ outflows. *Moore et al.* [1985] reported clear signatures of parallel velocity dispersion observed high over the dayside polar cap, leading to mass separation of the outflow, i.e., a geomagnetic mass spectrometer. *Lockwood et al.* [1985*b*] concluded that the dayside upwelling region below 1 R_E altitude is the source for these velocity dispersed higher altitude flows, which include significant O^+ content, as well as N^+, H^+, He^+, and O^{++}. The low-energy O^+ ions are convected far into the polar cap as they flow upward from the dayside auroral zone source, particularly during high magnetic activity [*Lockwood et al.*, 1985*b*; *Horwitz and Lockwood*, 1985].

The purpose of the present paper is to pursue the question as to the mechanisms responsible for the ion heating which defines the source region for these polar ion outflows. The general approach taken was to identify a typical upwelling ion event using the retarding ion mass spectrometer (RIMS) data, for which data would also be available from the other experiments on the DE 1 satellite, including energetic particles and magnetic and electric fields. Our intent is to bring all available information to bear on a representative event, thereby determining the characteristics of the upwelling ion source region. In practice, the choice of event was determined largely by the simultaneous availability of the several data sets.

Figure 1 displays the orbit of DE 1 for the upwelling ion event to be examined in detail here. Figure 1*a* is a plot of the trajectory in magnetic local time and invariant latitude. Note that the spacecraft starts in the polar cap and passes equatorward through the auroral zone into the plasmasphere on the dayside at about 1000 MLT. The upwelling ion event is observed between 1928 and 1935 UT (points 1 and 3 in Figure 1*a*), using the event definition adopted by *Lockwood et al.* [1985*a*]. Figure 1*b* provides a noon meridian plane view of the orbit between 1925 and 1935 UT.

[1] NASA Marshall Space Flight Center, Huntsville, Alabama.
[2] Rutherford Appleton Laboratory, Oxfordshire, England.
[3] University of Alabama at Huntsville.
[4] University of Iowa, Iowa City.
[5] NASA Goddard Space Flight Center, Greenbelt, Maryland.

Paper number 5A8713.
0148-0227/86/005A-8713$05.00

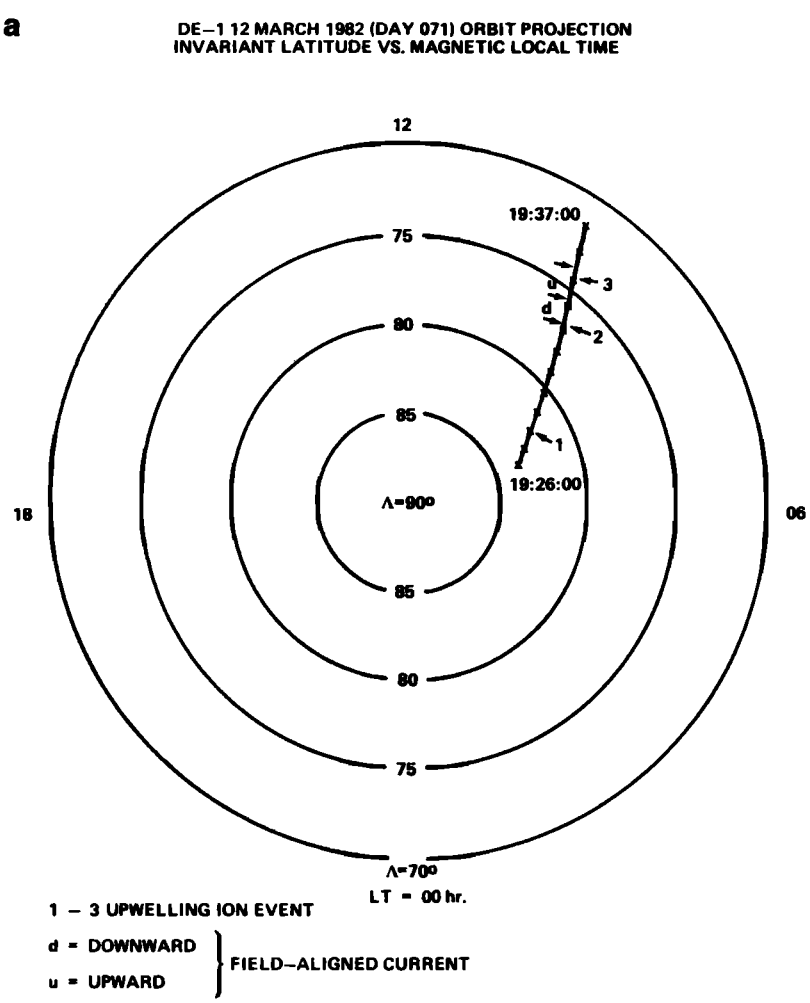

Fig. 1. Plots of DE 1 orbit for the data interval considered in this paper. (*a*) Magnetic local time versus invariant latitude, showing the track of the spacecraft conjugate point across the polar cap, through the dayside auroral zone. (*b*) Orbital projection in the noon-midnight meridian plane, showing the same motion. Arrows 1, 2, and 3 are the satellite locations at 1928, 1933, and 1935 UT; upwelling ions are observed between 1 and 3 and intense ion heating between 2 and 3.

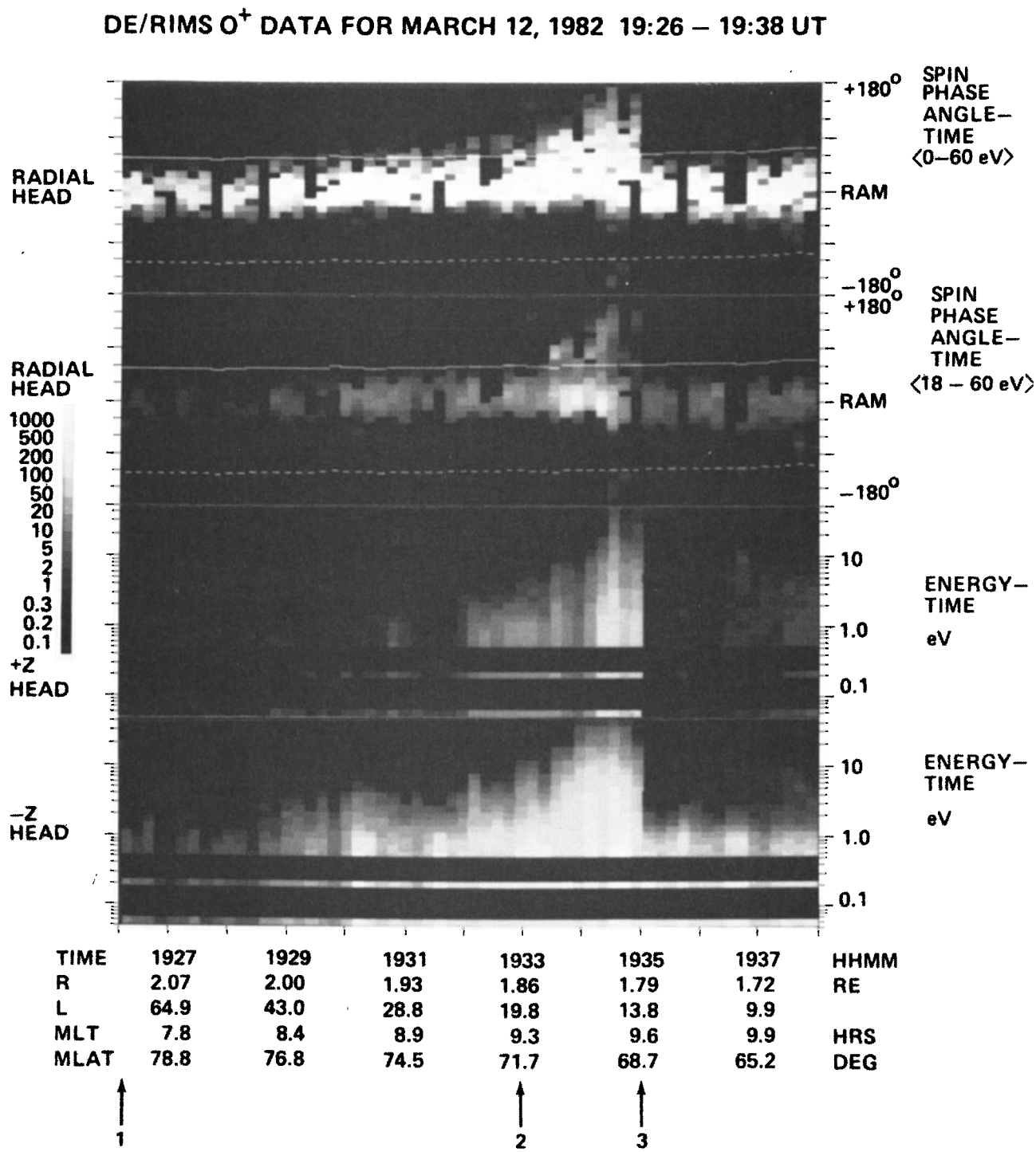

Fig. 2. DE 1 RIMS spectrograms from the radial and axial heads for the time period of the upwelling ion event 1925 to 1938 UT. Integral fluxes are color coded according to the color bar at the right of the figure. The top two panels show spin-time spectrograms of O^+ from the radial head averaged over two different energy ranges and the bottom two panels show retarding potential–time spectrograms of O^+ from the axial head.

Various aspects of upwelling ion events have been discussed by *Moore et al.* [1985], *Lockwood et al.* [1985*a*], and *Waite et al.* [1986]. The associated RIMS ion signature of the O^+ ion species for the event we focus on here is shown in Figure 2. Figure 2 is a multipanel figure showing the radial head data for O^+ in the top two panels in a spin phase angle versus time spectrogram format and the + and -*Z* head data (axial, transverse to line of flight), respectively, in the bottom two panels using a retarding potential versus time spectrogram format. The radial head data panels 1 and 2 are plotted as a function of the spin phase angle of the detector with respect to the satellite orbital direction on the vertical axis, time being on the horizontal axis. The spin axis of the spacecraft is normal to the spacecraft orbit and allows sampling of the full pitch angle range of the ions twice per spin. The upward and

downward field-aligned directions are marked on the plot by the dashed and dotted white traces, respectively. Note the upward excursion of the O^+ ion flux at 1928 with a dramatic equatorward cutoff at 1935 UT. The top panel indicates an average spin curve for all O^+ ions from 0 to 60 eV and panel two shows a spin curve for O^+ ions between 18 and 60 eV. Note that a conical ion signature emerges at the higher energies. The bottom two panels indicate the energy distribution of the plasma from 0 to 50 eV transverse to the orbital direction and to the magnetic field. The peak in the O^+ ion flux and associated energy distribution from 1934 to 1935 UT indicates the transverse ion heating taking place in the upwelling ion events.

The signature of upwelling ion events is indicative of strong heating of ionospheric H^+, He^+, and O^+ to temperatures of order 10^5 K. This heating signature for all ion species is easily visible in Figure 3, which displays retarding potential spectrograms of H^+, He^+, and O^+ for the upwelling ion events of Figure 2. These spectrograms are derived from the axial heads (transverse to line of flight) of the RIMS. The quantity contoured is the integral flux of ions entering the instrument aperture, i.e., the first energy moment of the ion species distribution function along the look direction and above the energy given by the sum of retarding potential and spacecraft potential. The axial heads view parallel and antiparallel to the spacecraft spin axis, perpendicular to the direction of flight and to the magnetic field direction. The axial head designated $+Z$ responds to westward traveling ions in the data plotted, while the $-Z$ head responds to eastward moving ions. Radial head data (see Figure 2), which scan the spin plane, show that O^+ ions enter the instrument mainly from the ram direction during the interval of Figure 3, with the exception of the upwelling event most obvious between 1933 and 1935 UT (points 2 and 3 in Figure 1*a*).

Note in Figure 3 the following features: (1) passage of the spacecraft toward lower altitudes and latitudes, across the dayside auroral oval or magnetospheric cleft region at local times near 1000 hours, (2) rapidly increasing H^+ and He^+ fluxes as the spacecraft enters the plasmasphere near $L = 4$, and (3) the upwelling O^+ signature, peaking at 1934–1935 UT, at $L = 14$, also present in the H^+ and He^+ spectrograms. The upwelling ion signature appears here as a localized region of ion outflux having an exceedingly high characteristic energy of order 10 eV. Each vertical strip of the spectrogram represents a retarding potential curve, the characteristic energy being given by the location in energy of the knee of the curve. The strongly heated population is observed in both axial heads, though there is an asymmetry between the heads, with larger fluxes observed by the $-Z$ head (i.e., of eastward traveling ions).

In the sections below, we will focus upon the upwelling event found at 1933–1935 UT in the spectrogram of Figures 2 and 3, examining in more detail the circumstances of the ion heating responsible for the widened angular distributions and extended energy distributions of the ions observed by RIMS.

PLASMA OBSERVATIONS

The operational mode of the RIMS instrument during this time period permits the direction derivation of the full O^+ distribution function in the range of energies up to 50 eV, without differentiation of retarding potential analyzer (RPA) curves. This capability results from the differential response of RIMS, with a full width at half maximum (FWHM) for O^+ of 14 eV. During the periods discussed here, the retarding grid potential remained at spacecraft potential, but the O^+ channel center energy was swept over the range from 0.05 to 50 eV. The energy resolution with which the distribution function is measured is rather coarse, however. Due to the width of the passband, the actual range of center energies is from 3.5 eV to 50 eV. Phase space densities can be derived from the detector count rates by use of known geometric response and the constant energy passband. The radial head samples the plane perpendicular to the spacecraft spin axis, with broad angular response lateral to that plane, while the axial sensor heads aligned parallel and antiparallel to the spin axis sample the distribution function not sampled by the radial head.

Plates 1*a*–1*d* display the two-dimensional O^+ distribution in the spin plane, as it evolves through this event, plotted in the velocity space of the spacecraft frame of reference. Initially (Plate 1*a*), we have a rather cold O^+ flow relative to the spacecraft, due largely to the ram motion of the spacecraft itself. An estimate of the O^+ temperature can be obtained by plotting phase space density versus energy measured from the peak location. The peak is nearly Gaussian (Maxwellian) with an *e*-folding energy (temperature) of approximately 0.8 eV. This is essentially the minimum resolvable temperature for this technique at an orbital speed of 7 km/s, so that this is an upper limit on the true temperature. A density estimate can also be made from the peak phase space density ($\sim 2.5 \times 10^{13}$ s^3 km^{-6}) and the volume of velocity space occupied ($\sim 9^3$ $(km/s)^3$). This leads to a value of some 2000×10^{13} km^{-3} or 20 cm^{-3}.

As the upwelling event begins (Plate 1*b*), heating becomes evident as increased contour spacing and conical lobes form which are roughly symmetric relative to the local magnetic field direction. Also, the O^+ density is increasing, to approximately 150 cm^{-3} at 1931 UT. At 1933–1934 (Plate 1*c*), well defined conical wings have formed on the core distribution, extending well beyond 50 eV (24 km/s O^+). Moreover, the distribution contains a side lobe separated from the main maximum, apparently at the root of one side of the conical wings. The density is at its greatest at this time, approximately 300 cm^{-3}. At 1934–1935 (Plate 1*d*), the core itself is significantly heated, and it is not as obvious whether well defined conical features exist, since much of the core distribution function extends beyond the RIMS energy sweep to 50 eV. At this time, the distribution is very nearly bi-Maxwellian with *e*-folding energies (measured again relative to the distribution peak location) of 3 eV in the direction upward along the magnetic field, and 11 eV perpendicular to the magnetic field. No structure is resolved within the core of the distribution in this interval. Equatorward of the event, the O^+ distribution returns to the relatively cold rammed form observed poleward of the event, but with a larger density of about 200 cm^{-3}.

Plate 2 presents energetic ion data from the energetic ion composition spectrometer (EICS). During the interval

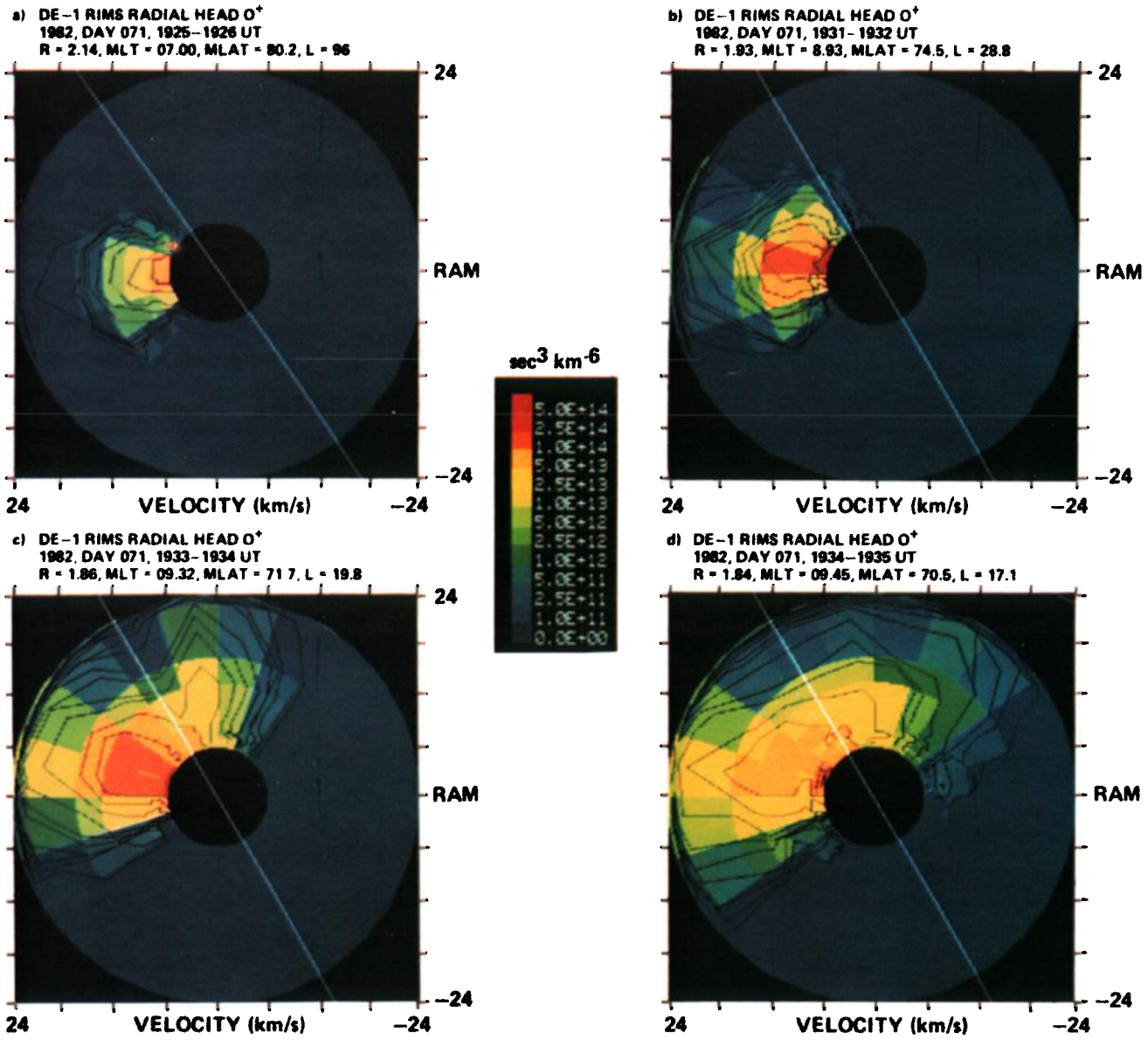

Plate 1. Spin plane O^+ distribution functions in the spacecraft velocity frame at four selected times throughout the upwelling event. (*a*) Prior to event, cold rammed O^+, apparently flowing opposite to spacecraft motion. (*b*) Some heating of the distribution becomes visible in directions perpendicular to the local magnetic field. (*c*) Pronounced formation of conical "wings" and a side lobe of the distribution core. (*d*) Pronounced transverse heating of the distribution core becomes evident, together with a very noticeable field-aligned asymmetry in the distribution corresponding to an upward heat flux.

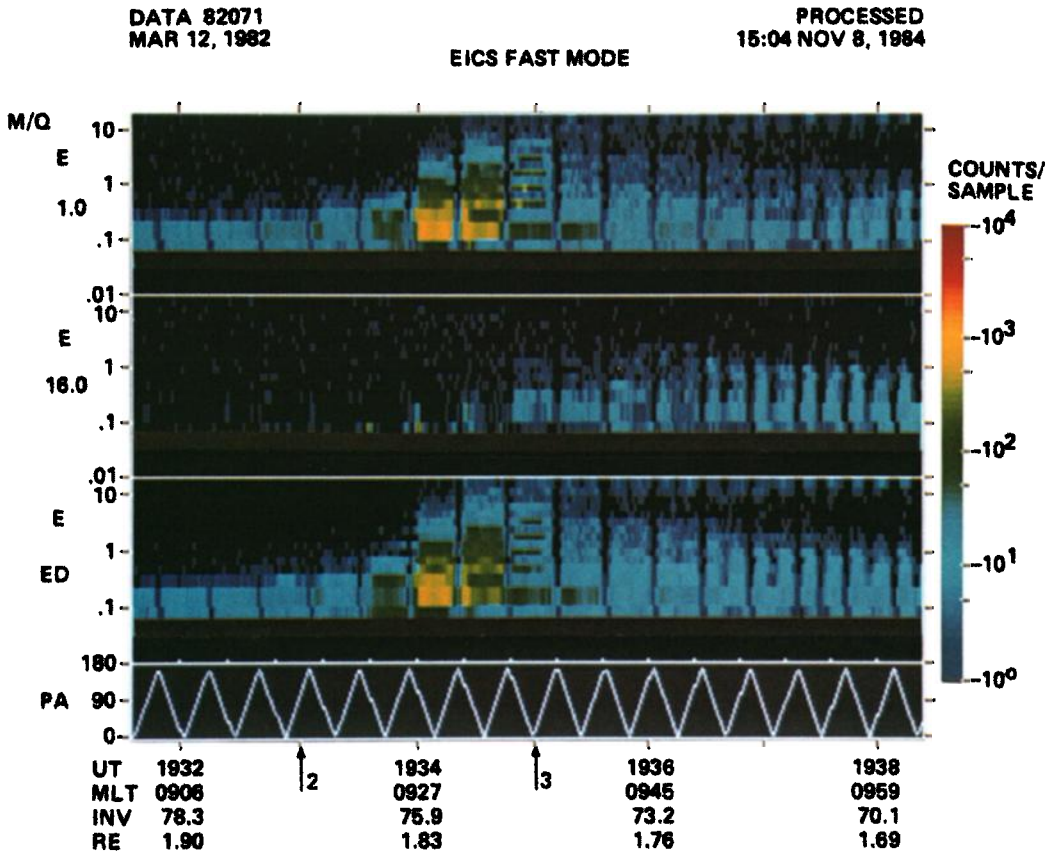

Plate 2. DE 1 energetic ion composition spectrometer spectrogram for the pass discussed here. Precipitating magnetosheath H^+ (with apparent loss cones) and upgoing low-energy O^+ (conic fluxes at lowest energy steps) are evident during the peak of the upwelling ion event (1933–1935 UT).

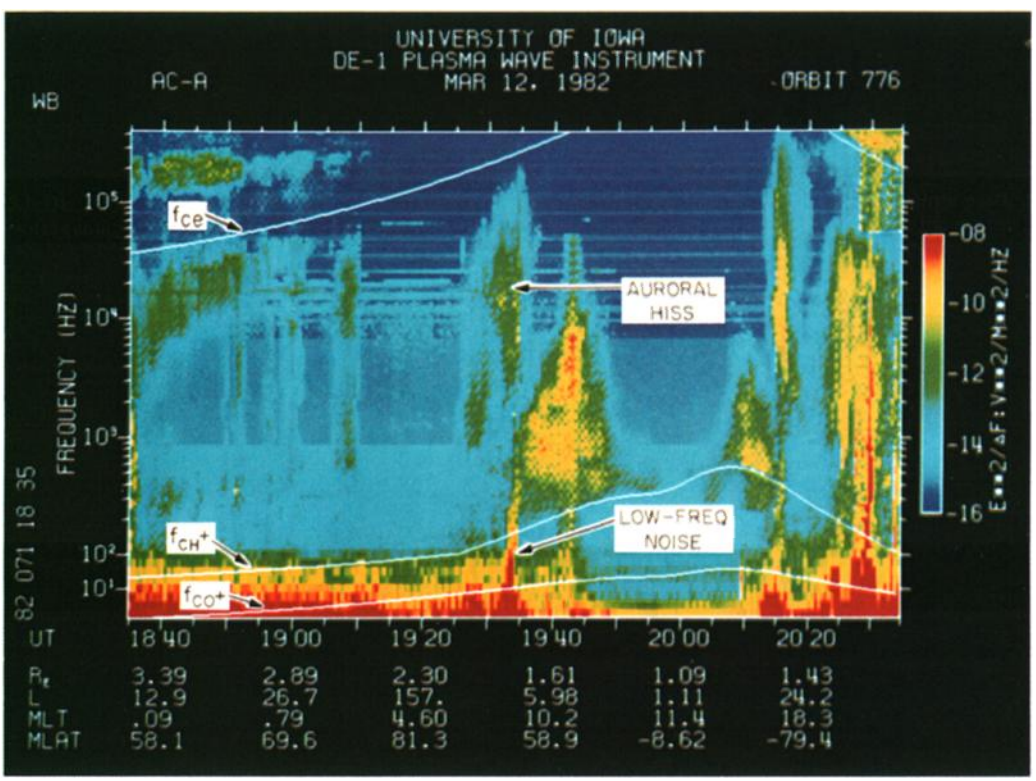

Plate 3. DE 1 plasma wave instrument observations of fluctuating fields during the upwelling event. Note particularly the low-frequency emissions associated with the peak of the event, appearing from 1 Hz to well above the proton gyrofrequency, marked by the labeled white trace. Other white traces mark oxygen and electron gyrofrequencies.

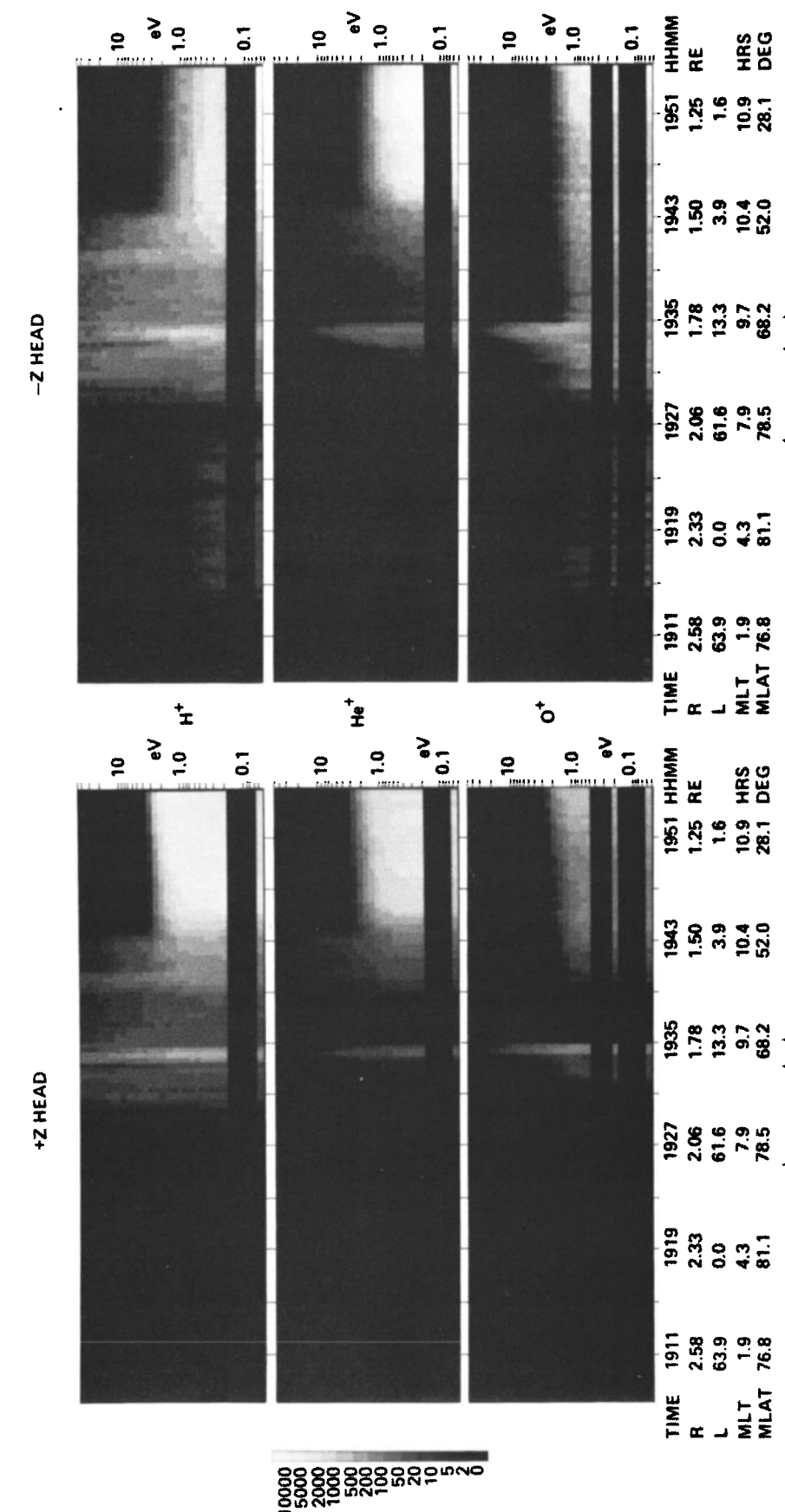

Fig. 3. DE 1 RIMS retarding potential spectrograms containing the segment of the orbit plotted in Figure 1. Integral fluxes are color coded for the retarding potentials indicated on the scales at the right side of the panels. Data are provided for O^+, H^+, and He^+ from each of the axial heads, +Z fluxes are westward, and −Z fluxes are eastward. Arrows 1, 2, and 3 in this and all other figures refer to the satellite locations given in Figure 1.

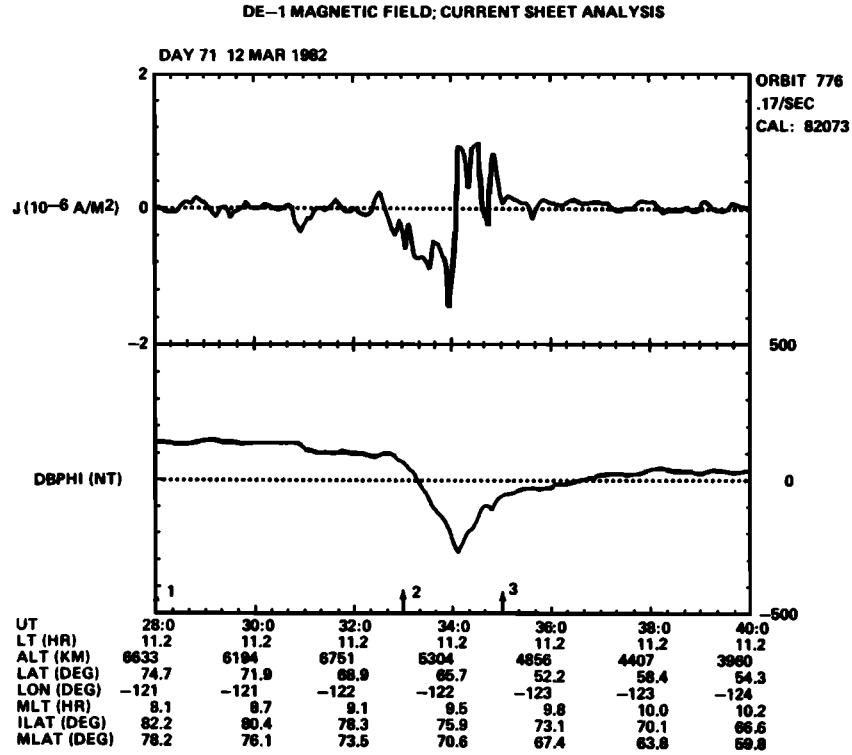

Fig. 4. DE 1 magnetometer signature for the upwelling event, showing interpretation in terms of two adjacent field-aligned current sheets having current densities of approximately 1 microampere/m^2 each.

shown in Plate 2, the EICS was operated in a mode which excluded ions with energies less than about 100 eV. The lowest energy channel is insensitive to ions with energies greater than 125 eV. The second energy channel, centered at 230 eV, has an energy full width at half maximum of 160 eV. The instrumental count rate, which is color-coded, is proportional to the ion number flux. The high energy tail of the upwelling ion event is clearly visible in the O^+ (middle) panel of Plate 2 between 1933 and 1935. These ions probably represent the tail of the upwelling O^+ distribution. Because of the broad energy channels and rapid (compared to the instrumental response time) time scale of the event, no meaningful measure of the energetic O^+ temperature for this event is possible. However, in view of the importance of the distinction between bulk and tail heating, a search is currently in progress for events which better lend themselves to RIMS/EICS comparisons.

The energy-latitude dispersion of H^+ (top panel) between 1933 and 1935 is consistent with injection of magnetosheath plasma into the magnetosphere on cusp field lines [*Burch et al.*, 1985; *Peterson*, 1985]. A detailed study of the relative occurrence of magnetosheath (cusp) plasma with upwelling ion events has not yet been completed. In the subauroral region (i.e., after 1936) a population of trapped H^+ and O^+ having two symmetric loss cones is observed.

Field-Aligned Current Signature

The magnetic field signature observed during this dayside auroral zone pass was mainly in the east-west (ϕ) component of the perturbation magnetic field, which was obtained by subtracting the Magsat model for the earth's internal field from the observed magnetic field. The ϕ component is shown in the lower panel of Figure 4. The observed magnetic field variation can be interpreted as being produced by field-aligned current sheets that are approximately parallel to dipole L shells. Current densities deduced under an assumption of infinite current sheets are plotted in the upper panel of Figure 4; the current density is measured positive when the current is upward. The field-aligned current region consists of a poleward region of predominantly downward current (region 1) and an equatorward region of predominantly upward current (region 2) with a boundary near invariant latitude 75.7° or at 1935:06 UT in time. The timing of the magnetic perturbation indicates that the equatorward edge of the upwelling O^+ event was coincident with the equatorward edge of the upgoing current sheet, but that the event extended throughout both the upward and the downward directed sheets (see Figure 1*a*). This association between the upwelling O^+ signature and the auroral current sheets is always observed [*Lockwood et al.*, 1985*a*], but there is no clear association of the O^+ heating with either current sense. Inspection of Plates 1*c* and 1*d* shows that considerable differences exist between the O^+ distribution function within the upgoing and downgoing current sheets. In particular, more pronounced conic wings and the side lobe of the core distribution appear to have been associated with the downward current sheet, while more heating of the core distribution was associated with the upgoing current sheet, However, due to the finite travel time of the ions from the heating region and the strong horizontal convection observed during the event, it is impossible to unambiguously associate a given current sense with particular features in the O^+ ion distribution.

PLASMA WAVE ENVIRONMENT

Plate 3 shows an electric field frequency-time spectrogram from the plasma wave instrument for the period of this upwelling ion event. Auroral hiss emissions of relatively low intensity extend from 1 kHz to just over 100 kHz, cutting off at frequencies below the electron cyclotron frequency. Cold plasma theory predicts that, in low density regions of the magnetosphere where the electron plasma frequency is less than the electron cyclotron frequency, these whistler mode emissions will be driven into resonance at the electron plasma frequency. Using a technique for deriving the electron density from the upper frequency cutoff of the auroral hiss emissions (described in detail by *Persoon et al.* [1983]) a density profile is obtained during the time of the upwelling ion event. Calculated densities increase from 100 ± 45 cm^{-3} at 1930 to 430 ± 194 cm^{-3} at 1934. Limitations of the technique have been discussed fully by Persoon et al. The large uncertainty in the density determination is primarily due to the low intensity of the auroral hiss emissions with respect to the background noise level near resonance, making it impossible to locate the upper frequency cutoff to an accuracy greater than ± 20%. This uncertainty in locating the upper frequency cutoff corresponds to an uncertainty in the density determination of ± 45%. The resulting densities are, however, consistent with the RIMS ion density analysis (see Figure 8). The density profile indicates that abrupt enhancements in the plasma density occur between 1930 and 1935 UT in connection with the ion heating observed by RIMS.

From 1933–1935, intense low-frequency emissions can be seen extending from the lowest frequency of 1 Hz to well above the proton cyclotron frequency at 140 Hz. Similar broadband electric field noise has been found to occur at low altitudes over both the evening and morning auroral regions. The noise is believed to be generated in a source region above 2 R_E and has an average Poynting flux directed downward toward the earth [*Gurnett et al.*, 1984]. Gurnett et al. have estimated the wave energy to be $\sim 2 \times 10^{-2}$ erg cm^{-2} s^{-1} for these emissions, providing a possible source of energy for the O^+ ions. Low-frequency emissions, extending from the lowest frequency band at 1 Hz up to well above the proton gyrofrequency, are evident in close association with the upwelling ion event. The interesting question is whether these waves are a conduit of energy from some source to the ambient heated ions, or whether they instead are driven by the ion distribution function itself.

Emissions seen poleward of the upwelling ion event at frequencies spanning the lower hybrid frequency (1928–1930) represent the poleward spread of the auroral hiss emissions. Because of the noticeably lower densities poleward of the event, these hiss emissions are probably associated with the outflow of low-energy ions. However, what appears to be a density cavity or trough region equatorward of the event is most probably due to the sensitivity of the receiver rather than a real effect. Auroral plasma depletions which are commonly seen in the nightside auroral zone are not frequently observed in the cusp. When density depletions are observed in the cusp, they are not large. Intense emissions below 10^4 Hz at 1940 have been clearly identified as plasmaspheric hiss.

ELECTRIC FIELD ENVIRONMENT AND DERIVED PLASMA FLOWS AND DENSITIES

In addition to the geophysical significance of electric field measurements to macroscopic magnetospheric processes, electric field measurements assume a central role in the derivation of plasma parameters from RIMS data in this event. This is because the RIMS radial head retarding potential failed to sweep as programmed subsequent to day 329 of 1981. Consequently, it is not possible to measure the energies of the light ion species. Though much can be inferred from the spin distributions of integral flux alone through use of a fitting procedure, such a procedure would be highly questionable in view of the distinctly non-Maxwellian character of the observed O^+ distributions. We have adopted a more straightforward approach using the transverse quasi-static electric field measurements from the plasma wave instrument (PWI) on DE 1 to provide plasma flow velocity transverse to the magnetic field, then using the plasma integral flux distribution to geometrically construct the flow velocity parallel to the magnetic field, in the process obtaining the total flow vector in the spin plane and a lower limit on the ion density and field-aligned flux. This procedure is discussed in more detail by *Olsen et al.* [1985].

The electric field measurements are shown in Figure 5, which provides electric field components parallel to the spacecraft spin axis (perpendicular to the spacecraft orbit, E_Z) and perpendicular to the magnetic field but in the spacecraft spin plane (E_{perp}). E_Z gives the orbital plane plasma convection velocity ("headwind") and shows the presence of antisunward flow at high latitudes. E_{perp} gives the lateral plasma convection velocity ("crosswind"), showing dawnward convection at high latitudes, changing to duskward flow at lower latitudes, with a particularly strong channel or jet of flow, approaching 100 mV/m or nearly 10 km/s at this altitude (1934 UT), coincident with the current sheet interface and the upwelling ion event. A polar plot of the derived horizontal drift vectors is shown in Figure 6.

The derived plasma outflow parameters are plotted in Figure 7. Note the following:

1. The field-aligned flow of all species is enhanced by the upwelling ion heat source. In particular, O^+ outflow is enhanced from essentially zero to several kilometers per second in the event. The light ion outflow is enhanced over the polar wind flow which can be seen both equatorward and poleward of the upwelling event. (Note that the H^+ velocity has been divided by 5 in the plot.)

2. The field-aligned outflux behaves similarly to the flow velocity, the event enhancing the polar wind flux of H^+ and He^+, and generating a comparable field-aligned flux of O^+.

3. It is not obvious what effect the upwelling heat source has on the ion species densities. However, the data are suggestive of density enhancements in all species since the density decline with increasing latitude established equatorward of the event seems to be reversed for all three species analyzed (see Figure 8 also).

Additional information on the density of the plasma during the upwelling ion event can also be derived from the auroral hiss cutoffs in the plasma wave spectrum discussed in the previous (plasma wave environment) section. The

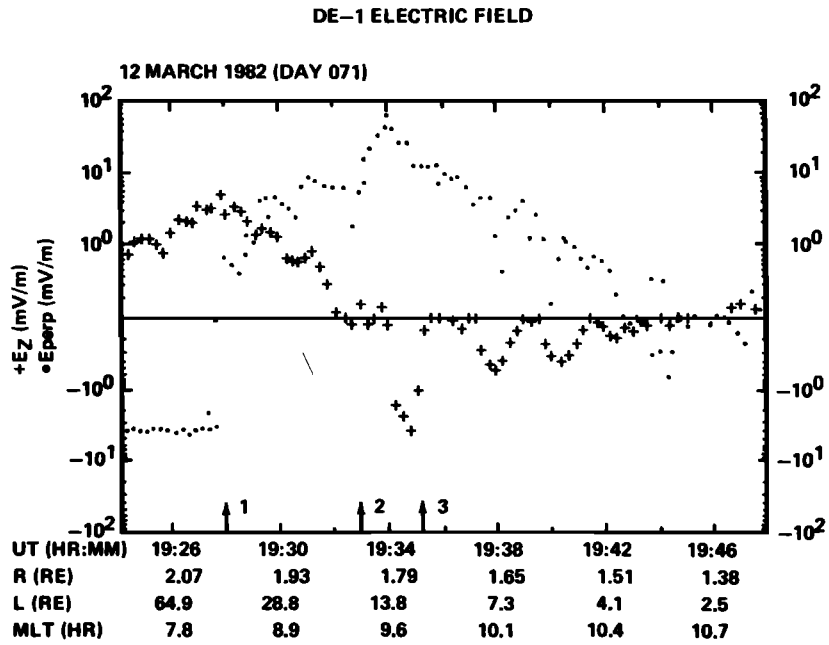

Fig. 5. DE 1 dc electric field for the upwelling ion event, showing the spin axis (E_z, headwind flow) component, and the perpendicular (E_{perp}, crosswind flow) component. Note the antisunward flow evolving into an intense eastward crosswind jet at the time of the upwelling ion event.

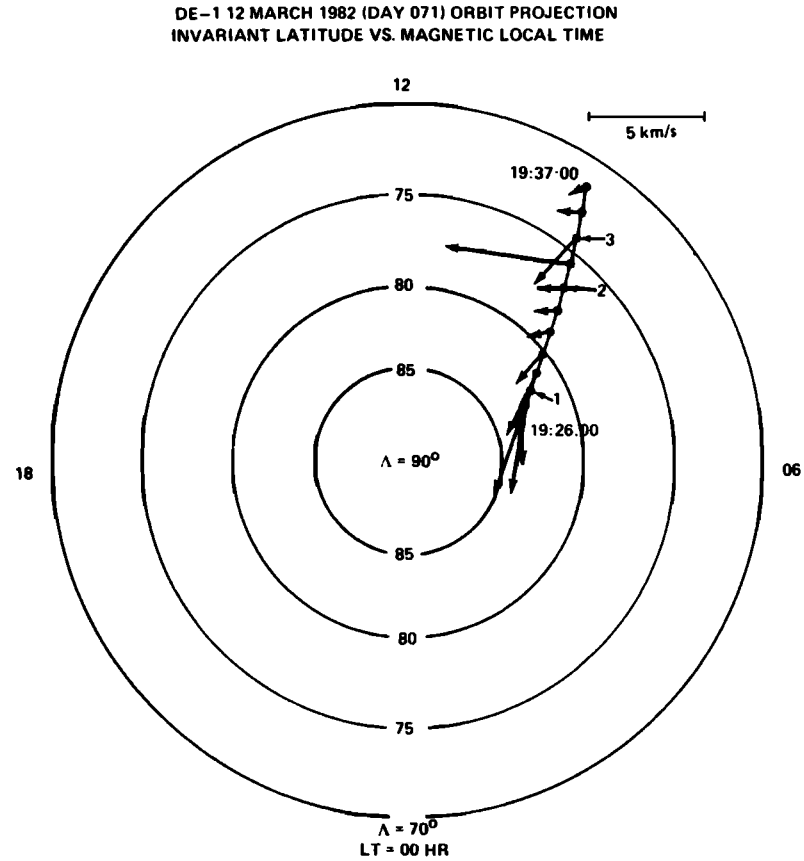

Fig. 6. A polar plot of the horizontal ion drift velocities calculated from the DE 1 dc electric field data of Figure 5. Note the antisunward flow evolving into an intense eastward crosswind channel at the time of the upwelling ion event.

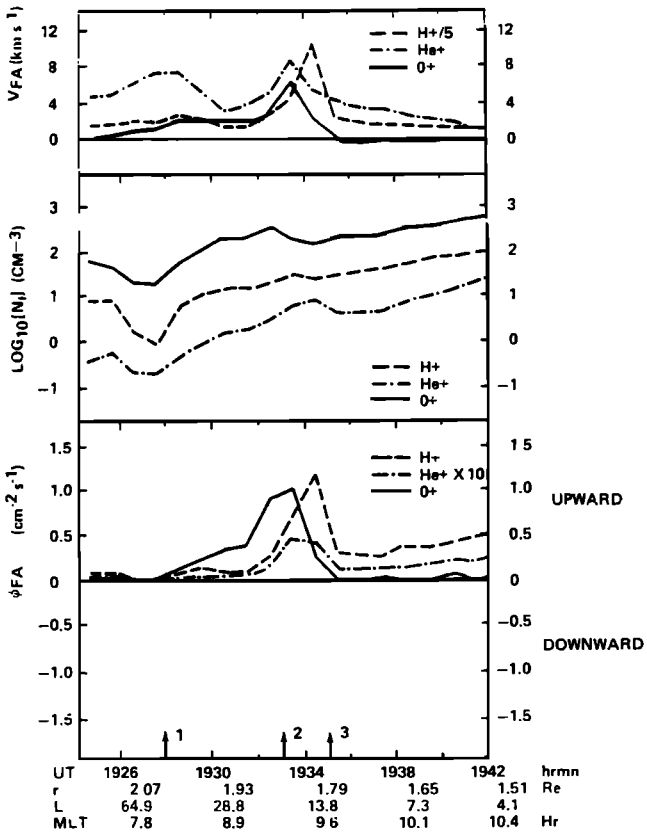

Fig. 7. Derived flow velocities, densities, and outfluxes for the RIMS ion flow observations, using, as input, the DE 1 electric field measurements (see Figure 5) for deconvolving spacecraft and plasma flow directions.

PWI derived densities and the RIMS derived total plasma density are plotted in Figure 8. There is relatively good agreement in the derived plasma densities and an indication of a true peak in the ion density during the upwelling ion event of 200 to 400 cm^{-3}. Also in Figure 8, we show the transverse O^+ ion temperatures, derived from the -Z axial head RPA data. The temperatures vary from 0.6 eV at 1926 UT to 7.2 eV at the peak of the event near 1935 UT. Note the general consistency with the radial head temperature inferences derived earlier. The H^+ transverse energy distribution at the peak of the event (1935 UT) however is highly non-Maxwellian with an energy distribution roughly comparable to the O^+, but with a highly extended high energy tail (see Figure 9). He^+ is fit reasonably well with a flowing Maxwellian with a temperature of 4.5 eV (Figure 9).

DISCUSSION

In this paper we have examined in detail the characteristics of an upwelling ion event exemplary of the source region for many of the polar ionospheric outflows which have recently been reported. The most notable features of this event include transverse ion heating to temperatures of order 10^5 K, large outward flow of the heavy ion O^+, enhanced outflow of light ions H^+ and He^+, moderately strong field-aligned current sheets of both senses, an associated intense eastward convection channel, and strong emission of waves in the frequency range near and below the proton gyrofrequency.

Models of ionospheric outflow [*Moore*, 1984, and references therein] have traditionally predicted relatively small escaping fluxes of O^+ when based upon escape of photoionization at typical ionospheric temperatures of a few thousand degrees Kelvin (polar wind solutions). Recently, the earlier models have been extended by the simple expedient of increasing the temperature of the electron gas to about 10^4 K [*Barakat and Schunk*, 1983]. Such electron temperatures are being found in the dayside auroral zone and cusp region at altitudes as low as 1000 km [*Brace*, 1984], in association with the energetic processes occurring there. Energy deposited into heating of the electron gas is communicated to the ion gas by the enhanced ambipolar electric field, and can overcome the gravitational trapping of a significant fraction of the O^+ ions, leading to larger O^+ escape flux than in the traditional polar wind.

Ion heating can influence the nature of ionospheric outflows in a more direct way than electron heating, since enhancements of the ambipolar electric field need not mediate the acceleration of ions to achieve an enhanced plasma flow. Large ion outfluxes produced by ion heating of the magnitude reported here have recently been modeled by *Gombosi et al.* [1985]. The model produced transient O^+ outfluxes of $>10^9$ cm^{-2} s^{-1}, sufficient to explain the observed ion outfluxes. Although these results are suggestive, further detailed modeling must be carried out to fully understand the upwelling ion outflow process.

The signature observed in this upwelling ion event suggests ion heating dominates the outflow energetics, especially in comparison with adjacent regions of light ion polar wind. We cannot exclude the possibility that electron heating is present and contributing to the field-aligned acceleration of the ions via the ambipolar field. However, the observed ion temperature is on the order of 10 times the recently observed electron temperature referred to above, sufficient to gravitationally free most or all of the O^+ present. Moreover, the observed outflow is at these altitudes more in the nature of a hot efflux than a supersonic beam, as expected when electron heating dominates.

The heating reported here has been anticipated to a great degree by earlier measurements of transverse ion heating restricted to energies greater than 5 to 10 eV [*Moore*, 1984, and references therein]. The contribution of the present work is in showing that, in the case of upwelling ions, there is in fact a bulk heating of the ionospheric plasma, and not merely the creation of an energetic tail on an otherwise cool distribution.

The most fascinating question raised by this and earlier studies is that of the energy source and mechanism of ion heating. The finding that hundreds, and at lower altitudes perhaps thousands, of ions per cubic centimeter are heated to temperatures of 10^5 K presents increased demands upon the required power of the heating mechanism. A crude estimate based upon a flux of 0.5×10^9 O^+ cm^{-2} s^{-1} at F region heights (namely, 10^8 O^+ cm^{-2} s^{-1} at 1.8 R_E, Figure 5) and an energy gain from 0.3 eV to 10 eV yields an energy flux of 0.3×10^{-5} W/m^2 (0.3×10^{-2} erg cm^{-2} s^{-1}). Though not large by auroral standards, this is indeed very large by polar wind standards.

As potential sources of energy for the ion heating, we have strong field-aligned currents, strong perpendicular

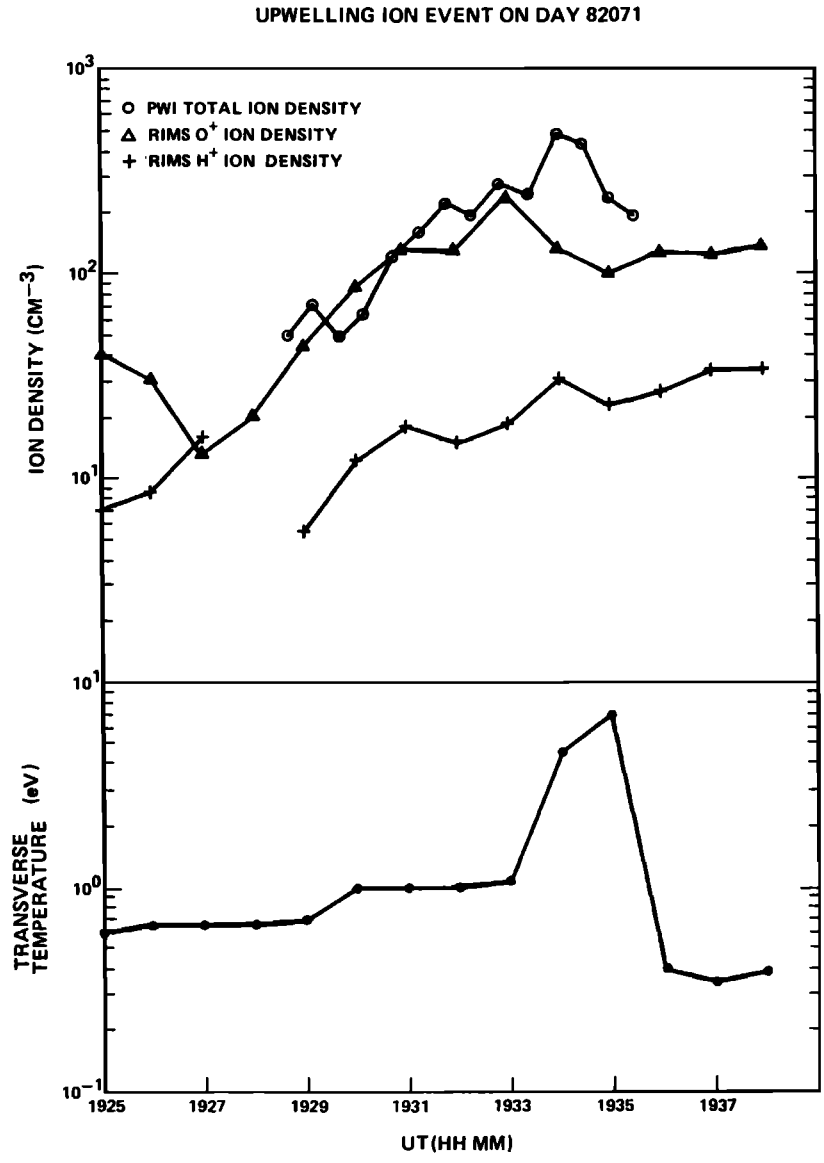

Fig. 8. The top panel shows the PWI and RIMS derived total plasma density. The second panel indicates the transverse O^+ ion temperature during the event derived from the -Z axial head using a drifting Maxwellian fit to the data.

electric fields associated with a plasma convection jet, and various wave emissions which may have propagated from a distant generation site, or may have been locally generated by plasma current or flow instabilities. We feel that the correspondence between the O^+ heating, its characteristic random energy (10 eV), and the flow energy of the convection jet for O^+, is highly suggestive of a collisional or Joule heating mechanism. However, it is not clear how such a mechanism can work at an altitude where there are ordinarily few collisions on time scales of interest or how the energy could be transported up from lower altitudes where such heating is strong.

CONCLUSIONS

The transverse ion heating in this upwelling ion event is closely linked to field-aligned currents and an associated auroral convection channel or jet. The strongest field-aligned flow enhancement was produced in the center of the jet. The heating associated with the poleward side (downward current) of the jet was associated with a conical feature in the tail of the O^+ distribution function and a side lobe of the core distribution. The heating associated with the equatorward side (upward current) of the jet was associated with more pronounced heating of the core of the O^+ distribution, with no resolvable structure. Comparison with energetic ion measurements indicates that the ion conic feature extended up to 100 eV and beyond, with no clear dependence upon current sense.

It may be concluded that heavy ion outflows observed in the polar magnetosphere and traced to a source in the dayside auroral zone are produced by marked transverse ion heating below 1 R_E altitude. The observed heating exceeds gravitational escape requirements independent of whether or not elevated electron temperature and enhanced ambipolar electric field reduce this requirement. Thus, in contrast with the emphasis of recent model results

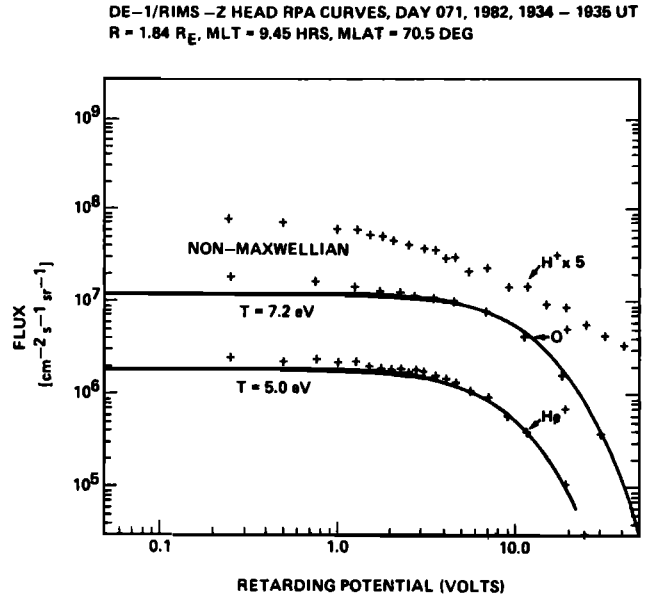

Fig. 9. The figure shows H^+, He^+, and O^+ integral RPA curves in the direction transverse to the magnetic field taken from the -Z axial head data near the peak of the upwelling ion event from 1934 to 1935 UT. A drifting Maxwellian fit to the data for O^+ and He^+ is shown by the solid lines.

[*Barakat and Schunk*, 1983], ion heating, rather than electron heating, appears to dominate the energetics of dayside auroral zone ion outflows. This leads to a hot subsonic flow from the source region rather than the cold supersonic flow associated with ambipolar electric field acceleration.

Acknowledgments. The authors are indebted to the engineering and science staff of the University of Texas at Dallas, to the RIMS team at MSFC, and to the programming staffs of Intergraph and Boeing Corporations for assistance with the data reduction software. Support for M. Lockwood and M. O. Chandler came from the National Research Council, under their Resident Research Associateship program, while partial support for M. O. Chandler came from NASA contract NAS8-33982 with the University of Alabama in Huntsville. Data from the energetic ion composition spectrometer on DE 1, as well as many helpful comments and suggestions on the manuscript, were provided by W. K. Peterson with the support of NASA contract NAS5-28710 to the Lockheed Missiles and Space Corporation. The work at the University of Iowa was supported by NASA contracts NAG5-210 and NGC-16-001-043. The authors would also like to express their gratitude for the use of computing and network facilities provided by the Data System Technology Program and the Space Physics Analysis Network.

The Editor thanks the two referees for their assistance in evaluating this paper.

REFERENCES

Barakat, A. R., and R. W. Schunk, O^+ ions in the polar wind, *J. Geophys. Res., 88,* 7887, 1983.

Biddle, A. P., T. E. Moore, and C. R. Chappell, Evidence for ion heat flux in the light ion polar wind, *J. Geophys. Res., 90,* 8552, 1985.

Brace, L. H., Planetary ionospheric energetics, paper presented at the Conference on Planetary Plasma Environments: A Comparative View, Stanford Univ., Yosemite, Calif., Feb. 1984.

Burch, J. L., P. H. Reiff, R. A. Heelis, J. D. Winningham, W. B. Hanson, C. Gurgiolo, J. D. Menietti, R. A. Hoffman, and J. N. Barfield, Plasma injection and transport in the mid-altitude polar cusp, *Geophys. Res. Lett., 9,* 921, 1982.

Burch, J. L., P. H. Reiff, J. D. Menietti, R. A. Heelis, W. B. Hanson, S. D. Shawhan, E. G. Shelley, M. Sugiura, D. R. Weimer, and J. D. Winningham, IMF B_y-dependent plasma flow and Birkeland currents in the dayside magnetosphere, 1, Dynamics Explorer observations, *J. Geophys. Res., 90,* 1577, 1985.

Gombosi, T., T. E. Cravens, and A. F. Nagy, A time-dependent theoretical model of the polar wind: Preliminary results, *Geophys. Res. Lett., 12,* 167, 1985.

Gurgiolo, C., and J. L. Burch, DE-1 observations of the polar wind--A heated and an unheated component, *Geophys. Res. Lett., 9,* 945, 1982.

Gurnett, D. A., R. L. Huff, J. D. Menietti, J. L. Burch, J. D. Winningham, and S. D. Shawhan, Correlated low-frequency electric and magnetic noise along the auroral field lines, *J. Geophys. Res., 89,* 8971, 1984.

Horwitz, J. L., and M. Lockwood, The cleft ion fountain: A two-dimensional kinetic model, *J. Geophys. Res., 90,* 9749, 1985.

Lockwood, M., J. H. Waite, Jr., T. E. Moore, J. F. E. Johnson, and C. R. Chappell, A new source of suprathermal O^+ ions near the dayside polar cap boundary, *J. Geophys. Res., 90,* 4099, 1985*a*.

Lockwood, M., M. O. Chandler, J. L. Horwitz, J. H. Waite, Jr., T. E. Moore, and C. R. Chappell, The cleft ion fountain, *J. Geophys. Res., 90,* 9736, 1985*b*.

Moore, T. E., Superthermal ionospheric outflows, *Rev. Geophys., 22,* 264, 1984.

Moore, T. E., C. R. Chappell, M. Lockwood, and J. H. Waite, Jr., Superthermal ion signatures of auroral acceleration processes, *J. Geophys. Res., 90,* 1611, 1985.

Olsen, R. C., R. H. Comfort, M. O. Chandler, T. E. Moore, J. H. Waite, Jr., D. L. Reasoner, and A. P. Biddle, DE 1 RIMS operational characteristics, *NASA Tech. Memo., TM-86527,* 1985.

Persoon, A. M., D. A. Gurnett, and S. D. Shawhan, Polar cap electron densities from DE 1 plasma wave observations, *J. Geophys. Res., 88,* 10,123, 1983.

Peterson, W. K., Ion injection and acceleration in the cusp, in *The Polar Cusp,* edited by J. A. Holtet and A. Egeland, pp. 67-84, D. Reidel, Hingham, Mass., 1985.

Shelley, E. G., W. K. Peterson, A. G. Ghielmetti, and J. Geiss, The polar ionosphere as a source of energetic magnetospheric plasma, *Geophys. Res. Lett., 9,* 941, 1982.

Waite, J. H., Jr., T. Nagai, J. F. E. Johnson, C. R. Chappell, J. L. Burch, T. L. Killeen, P. B. Hays, G. R. Carignan, W. K. Peterson, and E. G. Shelley, Escape of suprathermal O^+ ions in the polar cap, *J. Geophys. Res., 90,* 1619, 1985.

Waite, J. H., Jr., M. Lockwood, T. E. Moore, M. O. Chandler, J. L. Horwitz, and C. R. Chappell, Solar wind-magnetosphere coupling, in *Solar Wind-Magnetosphere Coupling,* edited by Y. Kamide and J. A. Slavin, Terra-Reidel, Kyoto, in press, 1986.

M. O. Chandler, Dept. of Physics, University of Alabama in Huntsville, Huntsville, AL 35899.

C. R. Chappell, T. E. Moore, and J. H. Waite, Jr., Space Science Laboratory, NASA Marshall Space Flight Center, Code ES53, Huntsville, AL 35812.

M. Lockwood, Rutherford Appleton Laboratory, Chilton, Didcot, Oxfordshire OX11 0QX, England.

A. Persoon, Dept. of Physics and Astronomy, University of Iowa, Iowa City, IA 52242.

M. Sugiura, NASA Goddard Space Flight Center, Code 696, Greenbelt, MD 20771.

(Received June 10, 1985,
revised September 9, 1985;
accepted November 11, 1985.)